Optimal Marching of Autonomous Networked Robots

Buri Ban, Miao Jin, and Hongyi Wu

The Center for Advanced Computer Studies, University of Louisiana at Lafayette, Lafayette, LA 70503.
{bxb7073,mjin,wu}@cacs.louisiana.edu

Abstract—The recent advances in sensors, actuators, robots, and mobile wireless communication technologies have accelerated interest in autonomous networked robots (ANRs), where the individual robots coordinate among themselves to complete a task, e.g., to explore or monitor a Field of Interest (FoI). By teamwork, which is especially important in complex tasks, ANR system expresses much more capacity than traditional static sensor networks. Existing work focuses on improving the coverage performance of a group of ANRs within a single FoI. In this research, we consider a group of ANRs that are instructed to explore a number of FoIs. After they complete a task at current FoI, they move to the next one, which may be far away from current one and the shape can also vary dramatically. Our research focuses on how to efficiently enable such transition. The ANRs must be able to redeploy themselves to desired positions in the new FoI based on distributed algorithms. Besides, to avoid unexpected event breaks network's integrity, the ANRs should preserve their local connectivities as much as they can and organize themselves as a whole network without any isolated nodes during the transition. Furthermore, considering energy consumption, such relocation algorithm should work at the cost of reasonable total moving distance. We study this problem and call it *optimal marching of autonomous networked robots*. The proposed algorithms guarantee global connectivity, and preserve local connectivities as much as possible at negligible cost of moving distance. Additionally, ANRs can automatically adjust their deployment density in the new FoI based on the requirements of various tasks or regions.

I. INTRODUCTION

The recent development in sensors, actuators, robots, and mobile and wireless communication technologies has enabled a paradigm shift in robotic systems, named autonomous networked robots (ANRs), where the individual robots coordinate among themselves to complete a task, e.g., to explore or monitor a Field of Interest (FoI). Such an ANR system is extremely valuable in situations where a traditional static sensor network fails or is inapplicable, for example, in disaster areas or toxic urban regions where sensor deployment cannot be performed manually, or hostile environment where sensors can be neither manually deployed nor air-dropped. On the contrary, ANRs can move to correct positions by themselves to provide the required coverage. Compared with the static sensor network that is deployed for a given FoI, an ANR system offers great flexibility to explore different fields as needed. Additionally, an ANR system is more reliable since the failure of an individual robot can be recovered by its peers.

Algorithms have been developed to enhance the performance of coverage from random initial positions of ANRs as an end result of robots movement. Virtual-force based algorithms [1]–[3] are among the earliest endeavors. The work in [4] enables an ANR system to arrange themselves to a regularly spaced square or rectangle lattice pattern by exploiting a common reference orientation. In [5], algorithms are proposed to discover the existence of coverage holes and then compute the desired target positions to move robots from densely deployed areas to sparsely deployed areas to increase the coverage. Later, in [6], [7], decentralized motion control algorithms are proposed to deploy an ANR system in the so-called triangular lattice pattern, namely a network of equilateral triangles within a given area that is proved optimal in terms of minimum number of sensors required for complete coverage of a bounded area. Centroidal Voronoi Diagram based algorithms [8]–[10] can also achieve the layout of an ANR system close to equilateral triangulation, at the same time, easily encoding optimal coverage and sensing policies into the utility function.

Existing research focuses on improving the coverage performance of a group of ANRs as an end result of robots movement within a FoI. In this research, we consider a group of ANRs that are instructed to explore a number of FoIs. After they complete the task at a FoI, they move to the next FoI. Our research focuses on how to efficiently enable such transition. The new FoI may be far away from the previous one and its shape can also vary dramatically. Of course, a complete map can be loaded into the memory of each ANR, but the ANRs must be able to redeploy themselves to desired positions in the new FoI based on distributed algorithms. An efficient relocation algorithm wants to minimize the total moving distance for reducing energy consumption. However, it is more important that the ANRs preserve their local connectivities and organize themselves as a whole network without any isolated nodes during the transition to the new FoI. The global connectivity requirement is mandatory in order to make sure timely coordination among the ANRs. For instance, an unexpected event (such as the change of terrain or weather conditions) may happen during the relocation. As a result, the ANRs must cooperatively determine how to adapt to the event. If an ANR is isolated at this time, it may be excluded from the new plan and thus become permanently lost. The preservation of local connectivity is also highly preferred to reduce the overhead and avoid the delay for pairing the wireless devices. Two ANRs can communicate with each other only if they are paired and have established a secure link. The extensive change of local connectivity may result in significant overhead and delay for re-pairing the wireless links, thus degrading the system performance and even hindering the system function.

We study this problem and call it *optimal marching of autonomous networked robots*. We assume a group of ANRs

initially deployed on a general 2D surface. They are required to redeploy to a new FoI, which is not necessarily close to the current one and may have complicated and concave boundary shapes, with inner obstacles or holes. The challenge to solve this problem is that it is impossible, as we prove in the paper, to preserve connectivities and minimize the total moving distance at the same time. To preserve connectivities, a straightforward approach is to keep robots move in a parallel way to a new FoI. However, this method would potentially produce longer total moving distance, and some robots may still get isolated if the new FoI has complex shape as mentioned above. To minimize the total moving distance, local connectivities will be dramatically broken during the movement and the global connectivity will also be an issue. We also prove in the paper that it is impossible to maintain all the local connectivities for general cases. Based on the insights from harmonic map, we propose a modified harmonic map algorithm to find moving path for each ANR to target FoI such that both local and global connectivities are maintained. Each ANR then follows a specified rule inside the target FoI to do minor adjustment towards its optimal coverage position. We show that the proposed algorithms guarantee global connectivity, and preserve local connectivities as much as possible at negligible cost of the total moving distance.

The main results and contributions of this work are summarized as follows:

- We formulate the optimal marching problem of a group of ANRs.

- We show that it is generally impossible to maintain all the local connectivities for a group of ANRs that are redeployed to a new FoI. We also show that it is a trade-off between preserving connectivities and minimizing the total moving distance to the desired coverage positions in the new FoI.

- We propose a series of distributed algorithms to solve the optimal marching problem. The proposed algorithms guarantee global connectivity, and preserve local connectivities as much as possible at negligible cost of the total moving distance.

- Additionally, ANRs can automatically adjust their deployment density in the new FoI based on the requirements of various tasks or regions.

The rest of the paper is organized as follows: Sec. II formulates the problem and reveals the insight of the proposed algorithms. Sec. III elaborates the proposed algorithms, followed by simulation results in Sec. IV. Sec. V concludes the paper and discusses our future work.

II. PROBLEM FORMULATION

We assume that an ANR system consists of a group of identical mobile robots. Each mobile robot has an equipped GPS and has the capacity to move in a straight line. The sensors mounted on mobile robots are assumed to have disk sensing model, identical sensing range and capability.

A. Optimal Marching Problem

Let there be n mobile robots in a known region - the current FoI denoted by M_1. Denote p_i the position of the ith mobile robot in M_1, and denote $P = \{p_1, \cdots, p_n\}$ the positions of the group of mobile robots in M_1. Following an instruction, the group of mobile robots moves to the target FoI denoted by M_2. They automatically redeploy themselves to optimal coverage positions in M_2 denoted by $Q = \{q_1, \cdots, q_n\}$.

Denote d_i the moving distance of the ith mobile robot from p_i in M_1 to q_j in M_2. The total moving distance of the group of mobile robots redeployed from M_1 to M_2 is defined as: $D = \sum_{i=1}^{n} d_i$.

Assume the total transition time from M_1 to M_2 is T. Denote $e_{ij}(t)$ the communication link between the ith and j^{th} mobile robots at time t. We assign a value to $e_{ij}(t)$ such that

$$e_{ij}(t) = \begin{cases} 1 & \text{if the } i^{th} \text{ and } j^{th} \text{ mobile robots } (i \neq j) \text{ are} \\ & \text{connected at time } t, 0 \leq t \leq T \\ 0 & \text{otherwise.} \end{cases}$$

Denote e_{ij} the communication link between the ith and j^{th} mobile robots during the whole transition time from M_1 to M_2. Similarly, we can assign a value to e_{ij} such that

$$e_{ij} = \begin{cases} 1 & \text{if } e_{ij}(t) = 1, \forall t, 0 \leq t \leq T \\ 0 & \text{otherwise.} \end{cases}$$

Then we can define the total stable link ratio to evaluate the preservation of local connectivity of a transition.

Definition 1 (Total Stable Link Ratio). Let there be n mobile robots relocating from the current FoI M_1 to the target one M_2. Denote m_i the number of neighbors of the ith mobile robot within its communication range in M_1. The total stable link ratio of the group of mobile robots relocating from M_1 to M_2, denoted by L, is defined as:

$$L = \frac{\sum_{i=1}^{n} \sum_{j=1}^{m_i} e_{ij}}{\sum_{i=1}^{n} m_i}.$$

We now can define the global connectivity of a group of mobile robots during a transition between FoIs.

Definition 2 (Global Connectivity). Let there be n mobile robots relocating from the current FoI M_1 to the target one M_2. The global connectivity of the group of mobile robots during the transition time T, denoted by C, is defined as:

$$C = \begin{cases} 1 & \text{given any mobile robot, there exists a path} \\ & \text{to network boundary for } \forall t, 0 \leq t \leq T \\ 0 & \text{otherwise} \end{cases}$$

The details of the above definition is addressed in Sec. III.

If we consider only the minimization of the total moving distance D during a relocation, we can show that the minimum moving distance marching problem can be converted to the well-known minimum cost bipartite matching problem and solved. Before we continue, we will first introduce some concepts of graph theory.

Definition 3 (Matching). Given a graph $G = (V, E)$ with a set V of vertices and a set E of edges, a matching $M \in E$ is a collection of edges such that every vertex of V is incident to at most one edge of M. If a vertex v has no edge of M incident

to it then v is said to be exposed. A matching is *perfect* if no vertex is exposed.

Definition 4 (Bipartite Graph). A graph $G = (V, E)$ is bipartite if the vertex set V can be partitioned into two sets V_1 and V_2 such that no edges in E has both endpoints in the same set of the bipartition. A bipartite graph G is balanced if $|V_1| = |V_2| = n$. The bipartite graph G is complete when there are all possible edges between V_1 and V_2.

Definition 5 (Minimum Cost Bipartite Matching Problem). Given a balanced and complete bipartite graph and a cost c_{ij} for all $e_{(i,j)} \in E$, find a perfect matching with minimum cost where the cost of a matching M is given by $c(M) = \sum_{e_{(i,j)} \in E} c_{ij}$.

Consider the positions of the group of mobile robots $P = \{p_1, \cdots, p_n\}$ in M_1 as the vertex set V_1, and the positions $Q = \{q_1, \cdots, q_n\}$ in M_2 as the vertex set V_2. We can construct a balanced and complete bipartite graph G. The cost associated with each edge is the Euclidean distance between the two incident vertices. The minimum moving distance problem equals to the minimum cost bipartite matching problem of G.

However, we show by the following Lemma that there is a contradiction between minimizing the total moving distance D and maximizing the total stable link ratio L.

Lemma 1. During the process of sensors moving from M_1 to M_2, maximizing stable link ratio L and minimizing total moving distance D cannot be achieved at the same time.

Proof: We can demonstrate the contradiction of maximizing L and minimizing D by an example given in Fig. 1(a).

Suppose M_1 is a slim rectangle shaped FoI along the x-axis. An optimal deployment of seven mobile robots in M_1 is to form a network of a triangular lattice pattern, namely a network of equilateral triangles as the one shown in the left in Fig. 1(a). Such way of deployment can achieve optimal area coverage in terms of minimum number of sensors required for complete coverage of a bounded region [11]. Furthermore, denote r_c the communication range, and r_s the sensing range. If $r_c \geq \sqrt{3} r_s$, every point in the region can be covered by at least one sensor, and every sensor is connected to six neighboring sensors [12]. In practice, the ratio of r_c/r_s has a wide range, not necessarily greater than $\sqrt{3}$. Given different values of k and r_c/r_s for different applications, the problem of determining the optimal deployment pattern that achieves both coverage and k-connectivity is still an open problem [13]–[15]. In this paper we only consider triangular lattice pattern for optimal coverage, so we have the assumption that $r_c \geq \sqrt{3} r_s$.

Suppose the FoI M_2 is also slim rectangle shaped, but along the y-axis. The optimal deployment of the same group of mobile robots in M_2 is the one shown in the right in Fig. 1(a). To maximize the total stable link ratio, we would choose a moving path with $\{A \to a, B \to b, C \to c, D \to d, E \to e, F \to f, G \to g\}$. However, to minimize the total moving distance, we would choose a totally different moving path with $\{A \to a, B \to g, C \to b, D \to e, E \to c, F \to f, G \to d\}$. ∎

Furthermore, the following Lemma shows that we cannot preserve all local links during relocation in general cases.

Lemma 2. The local connectivity cannot be fully preserved during relocation in general cases.
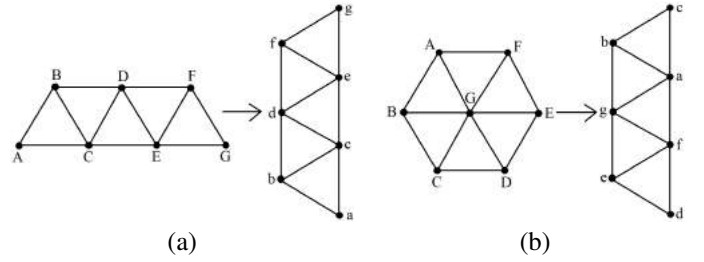

Fig. 1. Two examples of a group of mobile robots redeployed from one FoI to the other.

Proof: We still use contradiction to prove this Lemma. Assume we can preserve all local connectivities during relocation for general cases. Since we do not have restrictions on the shape of a FoI, we can construct one as illustrated in Fig. 1(b).

Suppose there are seven mobile robots deployed in M_1, a round shaped FoI. The optimal deployment for the seven mobile robots is one in the central, and the other six circled around to form a network of equilateral triangles as the one shown in the left in Fig. 1(b).

Suppose the FoI M_2 is slim rectangle shaped. The optimal deployment of the group of mobile robots in M_2 is the one shown in the right in Fig. 1(b). The centered mobile robot and two others circled around in M_1 have to break at least two communication links individually when they redeploy themselves to M_2. ∎

Considering both Lemmas 1 and 2, we formulate the optimal marching problem as the following one:

Definition 6 (Optimal Marching Problem). A group of ANRs are instructed to explore a number of FoIs sequentially. These FoIs are not necessarily close and may have complicated and concave boundary shapes with inner obstacles or landscape features that forbid mobile robot placement. The optimal marching problem is to maximize the total stable link ratio L subject to the requirement of the global connectivity $C = 1$ during the transition procedure between FoIs.

B. Our Method

We use a graph to model the connectivity of an ANR system. A vertex represents a mobile robot. An edge represents a communication link between two neighboring mobile robots. With position information of each mobile robot, we can easily extract a triangulation from such connectivity graph. Denote G the connectivity graph of a group of mobile robots deployed in M_1, and T the triangulation extracted from G. To redeploy the group of mobile robots from M_1 to M_2 with local connectivities, i.e., edges in T well preserved, basically we want to find a least stretched diffeomorphism of T mapped to M_2. A diffeomorphism is a one-to-one mapping keeping all local neighborhood relationship unchanged. A least stretched diffeomorphism preserves not just local neighborhood relationship but also edge lengths, which are crucial to keep local communication links unbroken during the transition.

To construct a least stretched diffeomorphism, we consider T as a spring system. Each edge is a spring with stretching

energy. We deform T such that the boundary of T is along the boundary of FoI M_2, and then let the vertices settle in equilibrium. Specifically, an inner vertex can move freely by stretching energy coming from its incident edges, while a boundary vertex can move only along the boundary edges. When the spring system is stable - none of the vertices is moving, the whole system achieves the minimum stretching energy. Such deformation is also called *discrete harmonic map*. Minimizing the spring stretching energy equals to minimizing the discrete harmonic energy. Discrete harmonic map is proved least-stretched and a guaranteed diffeomorphism with planar convex shape boundary condition [16], [17].

However, there exists a big challenge to directly apply discrete harmonic map method. The requirement of convex shape boundary is too restrictive on the shape of a FoI. In the paper we propose a modified harmonic map method. The basic idea is that instead of directly computing a diffeomorphism of T to M_2, we first compute two harmonic maps of T and M_2 to a unit planar disk respectively. Rotate either of the unit disks with an angle, the two overlapped disks induce a unique harmonic map between T and M_2. We find one optimal rotation angle such that the induced harmonic map gives the maximized total stable link ratio. A linear combination of the position of a mobile robot in M_1 and its mapped position in M_2 provides both the moving path and speed for the mobile robot. Each mobile robot then only needs a minor local adjustment inside M_2 to move to its optimal coverage position.

III. Our Algorithms

We take assumption that the communication range r_c and the sensing range r_s of a mobile robot satisfy $r_c \geq \sqrt{3}r_s$. The size of a FoI is bounded such that a system of ANRs can achieve full area coverage. We use Fig. 2 to visualize the major steps of the proposed algorithms when a group of mobile robots has finished tasks in current FoI M_1 and redeploy themselves to target FoI M_2. We first extract a triangulation denoted by T as shown in Fig. 2(b) from the connectivity graph of the group of mobile robots deployed in M_1 as shown in Fig. 2(a). A vertex represents a mobile robot, and an edge represents a communication link between two neighboring mobile robots. Fig. 2(c) shows the computed harmonic map of T to a unit disk. Fig. 2(d) shows the surface data of FoI M_2 with a flower-shaped pond inside. Similarly, we can easily grid and triangulate the surface data of M_2, and then harmonic map it to a unit disk. Rotate either of the unit disks with an angle, the two overlapped disks induce a unique harmonic map between T and M_2. We find one optimal rotation angle such that the induced harmonic map gives the maximized total stable link ratio. The group of mobile robots then follow the moving path and redeploy themselves to M_2 as shown in Fig. 2(e). After a minor local adjustment, each mobile robot moves to the computed optimal coverage position as shown in Fig. 2(f). We elaborate each step of the proposed algorithms in Sec. III-A, Sec. III-B, and Sec. III-C respectively. We also discuss some implementation issues in Sec. III-D.

A. Preprocessing

We apply the algorithm introduced in [18] to extract a triangulation denoted by T from the connectivity graph of the group of mobile robots deployed in M_1. With position information available at each mobile robot, each edge computes a weight that measures the number of triangles shared by the edge and the local neighbor sets of the edge. An iterative algorithm keeps removing edges based on current edge weight and local neighbor set information. The algorithm is fully distributed with computational complexity linear to the size of the edges.

B. Modified Harmonic Map

We first compute the harmonic map of T to a unit disk. Since a boundary edge incidents with only one triangle, we can easily identify the boundary edges of T. A boundary vertex with the smallest ID (a unique ID assigned to each mobile robot) initiates a message with a counter that records how many hops the message has travelled along the boundary. The starting vertex sends the message to one of its neighboring boundary vertices. The receiver updates the counter and records the number, and then forwards the message to its next neighboring boundary vertex. The message will come back to the starting vertex as the boundary vertices form a closed loop. The starting vertex notifies other boundary vertices the size of the boundary. Based on the recorded hop number and the size of the boundary vertices, each boundary vertex then computes a position along the boundary of a unit disk such that the boundary vertices are uniformly and sequentially distributed along the boundary. Inner vertices, i.e., non-boundary vertices, initiate their positions at the center of the unit disk. Then at each step, an inner vertex computes its position as the average of the positions of its neighboring vertices. Note that only inner vertices update their positions. We map T to the unit disk when no inner vertex updates its position and each vertex has a unique position in the unit disk. Similarly, we can add grid points and triangulate the surface data of FoI M_2, and then harmonic map it to a unit disk. The computation of the harmonic map of M_2 to a unit disk can be done by each mobile robot individually.

When T and M_2 are both mapped to unit disks, we can rotate either of the disks with any angle and the two overlapped disks induces a unique harmonic map between T and M_2. We want to find the optimal rotation angle such that the induced harmonic map gives the maximized total stable link ratio. However, it is a non-linear problem. To avoid complicated computation, each mobile robot applies a simple binary search method to find the desired rotation angle with a pre-defined search depth. At each step, a mobile robot divides current search interval of angle into two and rotates its mapped position in unit disk with the midpoint angle of the interval. The mobile robot computes its mapped position in M_2 and exchanges the position with its one-range neighbors. After calculating its own stable link ratio, the mobile robot then floods the information to other mobile robots. We set the search depth to 4 in our simulations in Sec. IV. The computed rotation angle has been very close to the optimal one with the search depth value.

After we rotate one mapped disk with the computed optimal rotation angle, the two overlapped unit disks naturally induce a harmonic map between T and M_2. Specifically, a vertex of T, denoted by v, locates three nearest grid points of M_2 in the overlapped unit disks. Denote g_i, g_j, and g_k the three nearest grid points, and $q(g_i)$, $q(g_j)$, and $q(g_k)$ the original geographic coordinates of g_i, g_j, and g_k in M_2. Denote
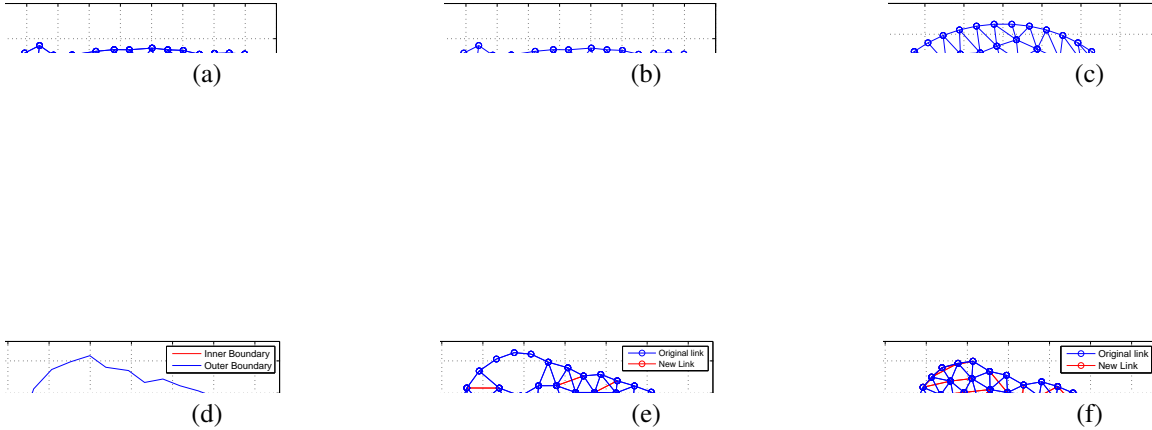
Fig. 2. Algorithm pipeline: (a) The connectivity graph of a group of mobile robots deployed in FoI denoted by M_1. (b) A triangulation denoted by T extracted from the connectivity graph. (c) The computed harmonic map of T to a unit disk. (d) The surface data of FoI denoted by M_2 with a flower-shaped pond inside. (e) The group of mobile robots follow the moving path of the harmonic map and redeploy themselves to M_2. (f) After a minor adjustment, each mobile robot moves to the optimal coverage position. Note that blue color marked edges represent local communication links preserved during the transition from M_1 to M_2. Red color marked edges, on the contrary, are new communication links.

(t_1, t_2, t_3) the Barycentric Coordinates of v in the triangle formed by g_i, g_j, and g_k when mapped to unit disk. [1] The linear combination

$$q(v) = t_1 q(g_i) + t_2 q(g_j) + t_3 q(g_k), \qquad (1)$$

gives the geographic coordinates where the mobile robot, represented by v, should deploy itself in M_2. Denote $p(v)$ the geographic coordinates of v in M_1, T the transition time of the group of mobile robots from M_1 to M_2, and t a time parameter. A linear combination of $p(v)$ and $q(v)$ with t:

$$\frac{T-t}{T} p(v) + \frac{t}{T} q(v), t \in [0, T] \qquad (2)$$

gives the mobile robot both the moving path and speed to M_2.

C. Minor Local Adjustment

After the group of mobile robots redeploy themselves to M_2, they only need a minor local adjustment to optimal coverage positions. We adopt *centroidal Voronoi diagram* based algorithms [8]–[10], [19] to compute optimal coverage position. Informally speaking, a Voronoi diagram is a partition of the space according to the distances to a discrete set of objects, denoted by sites such that a Voronoi region of a site is the region of points that are closer to the site than to any other sites. A centroidal Voronoi diagram is a Voronoi diagram such that each site is located at exactly the mass centroid of its corresponding Voronoi region with respect to a given density function. As proved in [20], centroidal Voronoi diagram always has congruent regular hexagons as its Voronoi regions in $R2$

---

[1]Please check Appendix for the definition of Barycentric Coordinates.

space, which induces a layout of sites forming equilateral triangulation.

Considering the group of mobile robots as sites, and the FoI M_2 as the partition space. We apply Lloyd algorithm [21], [22] to compute the centroidal Voronoi diagram. Lloyd algorithm is an iterative method. At each step, a mobile robot collects the position information of its two-range neighbors, computing its corresponding Voronoi region and the centroid of the Voronoi region. The mobile robot then moves to the centroid position. Since mobile robots have already been very close to the optimal coverage positions after redeploying to M_2, Lloyd algorithm only needs a few steps to converge when no mobile robot needs to update its position.

D. Discussions

1) Global Connectivity: If the shapes of the two FoIs M_1 and M_2 differ too much, some edges of T will be largely stretched when T is mapped to M_2 even though harmonic map is already a least stretched diffeomorphism. Such a largely stretched edge means a broken communication link between the two mobile robots represented by the two ending vertices of the edge. It is possible that all communication links of a vertex will be broken and the vertex will be isolated from the network.

To guarantee global connectivity during the transition procedure, we need a few modifications of the proposed modified harmonic map algorithm in Sec. III-B. Right after computing the harmonic map of T to M_2, a straightforward solution is that each mobile robot exchanges its mapped position with its one-range neighbors and checks whether all of its communication

links will be broken. For an isolated vertex, it chooses the closest one-range neighbor as reference and adjusts its moving path to M_2 parallel to the path of the neighbor and with the same speed.

However, in extreme case, a subgroup of mobile robots instead of a single one will get disconnected from the network. Considering that boundary vertices of T are mapped to the boundary of M_2 and form a closed loop, it is easy to check and require that the boundary vertices of T are still connected when mapped to M_2. A boundary vertex of T compares the mapped positions of its one-range neighbors with itself and initiates a packet with a counter set to zero to its one-range neighbors with communication links still preserved in M_2. If there exists at least a communication path connecting a vertex and a boundary vertex when mapped to M_2, the vertex will receive such a packet. When a vertex receives a packet from a boundary vertex that is further away from its current nearest boundary vertex, it stops forwarding this packet. Otherwise, the vertex updates the counter and record the number. Similarly, the vertex forwards the package to its neighbors with communication links still preserved in M_2. Assume the boundary vertices initiate their packages at approximately the same time, and each packet travels at approximately the same speed, the flooding of such packets in the network will then stop quickly depending on the diameter of the network. As a result, we can identify the isolated subgroups vertices.

For each isolated subgroup vertices, we choose a vertex with one of its one-range neighbors not just connecting but also nearest to a boundary vertex and set the vertex as root of the isolated subgroup vertices. The root vertex will then choose the neighbor as reference and adjusts its moving path to M_2 parallel to the path of the neighbor and with the same speed. The root will broadcast its moving path and speed to the subgroup vertices. Each vertex inside the subgroup will then adjust its moving path parallel to the path of the root one and with the same speed.

After the group of mobile robots redeploy themselves to M_2, we also need to guarantee global connectivity at each step of Lloyd algorithm when a mobile robot moves to the updated centroid position. At each step, a mobile robot collects the computed centroid positions of its one-range neighbors and compares with its own. If no mobile robot will disconnect from the network, every robot simply moves to its centroid position; otherwise, each robot checks whether it is safe to move to half of the distance to the centroid position and so on.

2) Moving Distance : As we have proved in Lemma 1, it is a contradiction between minimizing the total moving distance and maximizing the total stable link ratio during the relocation of a group of mobile robots. Although the proposed algorithm targets the optimal marching problem, maximizing the total stable link ratio, we can modify the proposed algorithm slightly to find transition paths with less total moving distance with the cost of a little bit lower of the total stable link ratio. When T and M_2 are both mapped to unit disks, we want to find an rotation angle such that the induced harmonic map gives the moving path of a group of mobile robots with the minimized total moving distance. Similarly, each mobile robot divides current search interval of angle into two and rotates its mapped position in unit disk with the midpoint angle of the interval.

The mobile robot computes its mapped position in M_2 and the moving distance to the mapped position, and then floods the distance information to other mobile robots. We can also set the search depth to 4.

3) Holes : A FoI can have complex shape. It may also contain obstacles or landscape features that forbid mobile robot placement. For simplicity, we call them holes of a FoI.

Harmonic map assumes not just convex boundary condition of the target FoI, but also topological disk shape for both current and target FoIs. For a FoI with holes, we cannot directly compute its harmonic map to a unit disk. A solution is to add a virtual vertex for each hole and fill all holes with virtual triangulations. Specifically, we apply the rule that a boundary edge incidents with only one triangle to detect boundary vertices along an inner hole. The position of an virtual vertex assigned to the hole is computed as average of the positions of boundary vertices along the hole. Each boundary vertex along the inner hole stores the position of the virtual vertex and adds one virtual edge connecting to it. At each step of harmonic map, boundary vertices along the inner hole exchange information to compute updated position of the virtual vertex.

With all holes filled with virtual triangulation, we can construct the harmonic map from T to M_2 as introduced in Sec. III-B. Note that it is possible that a mobile robot in T is mapped to a hole in M_2. The robot can simply choose the nearest grid point in M_2 as the mapped position. It is also possible that the moving path of a mobile robot computed by Eqn. 2 passes through a hole. When the mobile robot hits the boundary of the hole, the robot goes along the boundary until it can follow its computed moving path again.

A FoI with holes can also affect the computation of the centroidal Voronoi diagram. At each step, if the computed centroid falls into a hole, we choose the nearest grid point along the hole boundary as the centroid. It is also possible that a mobile robot hits a hole when moving to the computed centroid. Similarly, the robot goes along the boundary of the hole until it can follow the straight line to the computed centroid.

IV. Performance Evaluation

We test on models of FoI with different shapes and conduct extensive simulations to evaluate how well our algorithms perform. The parameters to evaluate the performance include the total stable link ratio, the total moving distance, and the global connectivity. The scenarios for testing include marching of a group of ANRs from a non-hole FoI to a non-hole FoI, a non-hole FoI to a FoI with holes, and a FoI with holes to a FoI with holes. We implement our algorithms in two versions. One version, represented by our method (a), maximizes the total stable link ratio subject to the requirement of the global connectivity during the transition. The other version, represented by our method (b), sacrifices a little total stable link ratio to achieve a less total moving distance.

Additionally, we implement two different methods for comparison. One method, represented by direct translation, computes the centroids of both the current and target FoIs M_1 and M_2 and a rigid translation from the centroid of

M_1 to the centroid of M_2. The mobile robots move from M_1 to M_2 based on the rigid translation, and then adjust themselves to optimal coverage positions in M_2 based on Hungarian method [23]–[25]. The other method, represented by Hungarian method, directly applies Hungarian algorithm to find the moving path of the group of mobile robots from M_1 to the optimal coverage positions in M_2, which should achieve the minimum total moving distance among all possible methods. For the two comparison methods, we assume the mobile robots have computed the optimal coverage positions in M_2 before the transition procedure.

A. Non-Hole to Non-Hole Scenarios

We first consider some relatively simple scenarios where both FoIs, M_1 and M_2, have no hole inside.

For the first scenario, the current FoI M_1 given in Fig. 2(a) has size $308,261$ m^2 with 144 mobile robots deployed. We assume the communication range of a mobile robot is 80 m. The target FoI M_2 shown in the first row of Fig. 3(a) has size 289745 m^2. The second row of Fig. 3(a) shows the connectivity graph of the group of mobile robots redeployed to M_2 following the path computed by our method (a). Note that blue color marked edges represent local communication links preserved during the transition from M_1 to M_2. Red color marked edges, on the contrary, are new communication links in M_2. The third row of Fig. 3(a) shows that the group of mobile robots have adjusted themselves to the optimal coverage positions in M_2. It is obvious that the positions of mobile robots have been very close to the optimal coverage positions after harmonic map. Therefore the moving cost in the minor adjustment step as introduced in Sec. III-C is low. The fourth and fifth rows of Fig. 3(a) compares the performance of our algorithms with others. We first compare the total moving distance. Since Hungarian method achieves the minimum total moving distance, we compare direct translation method and ours with Hungarian method. Note that we have included the adjustment cost of mobile robots in Sec. III-C into our methods. The forth row of Fig. 3(a) shows that as the distance between M_1 and M_2 increases, ranging from $10\times$ to $100\times$ communication ranges, the total moving distances of all methods converge to Hungarian method, but our methods always achieve less moving distance compared with direct translation method. It is obvious as shown in the fifth row of Fig. 3(a) that our methods can preserve most of the local communication links, which saves a lot of energy on updating new connections and benefits the network for security reasons.

The second scenario shares the same FoI M_1 given in Fig. 2(a). The FoI M_2 shown in the first row of Fig. 3(b) has size 173057 m^2. Compared with the first scenario, the boundary shapes of M_1 and M_2 in the second scenario differ a lot, so we can see an increased total moving distance for direct translation method in the second scenario. As for the total stable link ratio, our methods still performs much better than others.

B. Non-Hole to Hole Scenarios

We then consider more complicated scenarios where the FoI M_2 has inner holes. We still assume the FoI M_1 given in Fig. 2(a). The FoI M_2 in the third scenario has size 239987

Fig. 4. The performance of the proposed algorithms on target FoI model shown in Fig. 2(d). (a) The comparison of the total moving distance of our methods with others. (b) The comparison of the total stable link ratio of our methods with others.

m^2 with a concave hole inside as shown in Fig. 2(d). Fig. 4 gives the comparison of the performance of our methods with others for this scenario. The FoI M_2 in the forth scenario has size 233342 m^2 with a big convex hole inside as shown in the first row of Fig. 3(c). The FoI M_2 in our fifth scenario has size 253578 m^2 with multiple small holes inside as shown in the first row of Fig. 3(d). The comparison of both scenarios is still given in the forth and the fifth rows of Fig. 3(c) and (d) respectively.

The FoIs M_2 in the three scenarios share similar sizes and boundary shapes with M_1. As we can see that such similarity benefits the direct translation method, which reduces the total moving distance. However, our method still achieves less the total moving distance and the highest total stable link ratio among all comparison methods.

C. Hole to Hole Scenarios

The more complex scenarios are both M_1 and M_2 with complicated shapes and inner holes as shown in Fig. 5. In the sixth scenario, the FoI M_1 is deployed with 144 mobile robots as shown in the first row of Fig. 5(a). In the seventh scenario, the FoI M_1 is also deployed with 144 mobile robots as shown in the first row of Fig. 5(b). Similarly, The second row of Fig. 5 shows the connectivity graphs of the group of mobile robots redeployed to M_2 following the path computed by our method (a). The third row of Fig. 5 shows the optimal coverage positions of the group of mobile robots in M_2. The fourth and fifth rows of Fig. 5 compare the performance of our methods with others.

It is obvious that our methods still achieve less the total moving distance and the highest total stable link ratio among all comparison methods.

D. Global Connectivity

Table I shows the status of the global connectivity of a network during the transition procedure. Our proposed methods always maintain the global connectivity of the network, while it is highly possible for the other two methods that some mobile robots lose communication with neighbors and are isolated from the network during the relocation.

E. Adjusted Deployment Density

We can encode sensing policies or task requirements into the computation of the centroid of a Voronoi region in
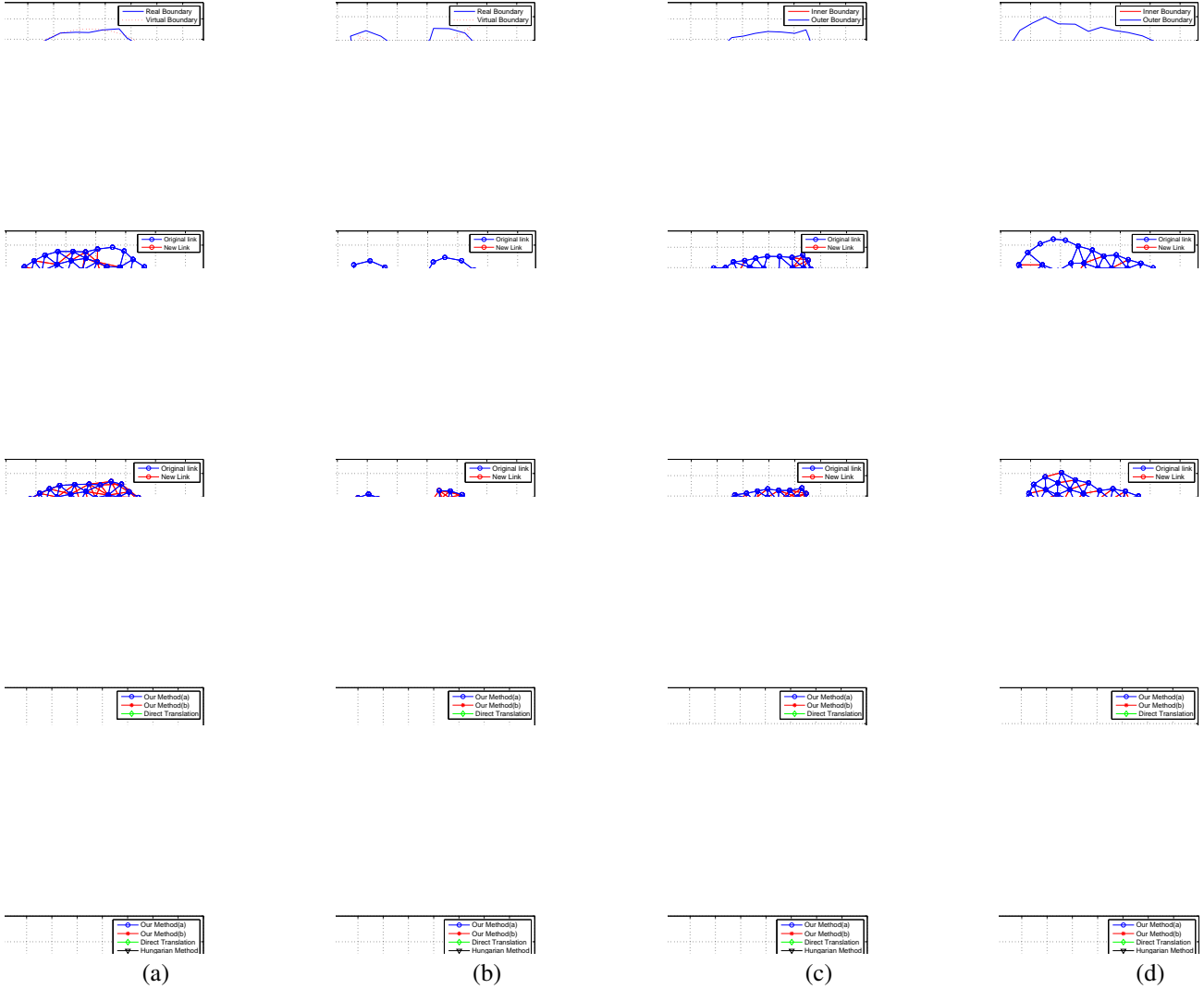
Fig. 3. The performance of the proposed algorithms on various target FoI models. The first row shows the surface data of different FoIs. The second row shows the connectivity graphs of a group of mobile robots redeployed in target FoIs following the paths computed by our method (a). Blue color marked edges represent local communication links preserved during the transition to a new FoI. Red color marked edges, on the contrary, are new communication links. The third row shows the connectivity graphs after mobile robots move to optimal coverage positions in target FoIs. The fourth row compares the total moving distance of our methods with others. The fifth row compares the total stable link ratio of our methods with others.

TABLE I.   GLOBAL CONNECTIVITY DURING TRANSITION PROCEDURE

	Our Method (a)	Our Method (b)	Direct Translation	Hungarian
Scenario 1	Y	Y	Y	N
Scenario 2	Y	Y	N	N
Scenario 3	Y	Y	Y	N
Scenario 4	Y	Y	Y	N
Scenario 5	Y	Y	Y	N
Scenario 6	Y	Y	N	N
Scenario 7	Y	Y	N	N

Sec. III-C, such that mobile robots can automatically adjust their deployment density inside target FoI. For example, we can add the temperature into the density function when com-puting the centroid of a Voronoi region, so more robots will be deployed near the center of a fire with higher temperature, while less robots in regions far away from the fire. Fig. 6 shows the modified forth scenario. A group of mobile robots with size 144 redeploys themselves from FoI M_1 given in Fig. 2(a) to FoI M_2 given in Fig. 2(d). We add the requirement that the closer to the hole, the more mobile robots are needed.

V.   CONCLUSION AND FUTURE WORKS

We study the optimal marching problem in the paper. After a group of mobile robots finishing task on current FoI, they
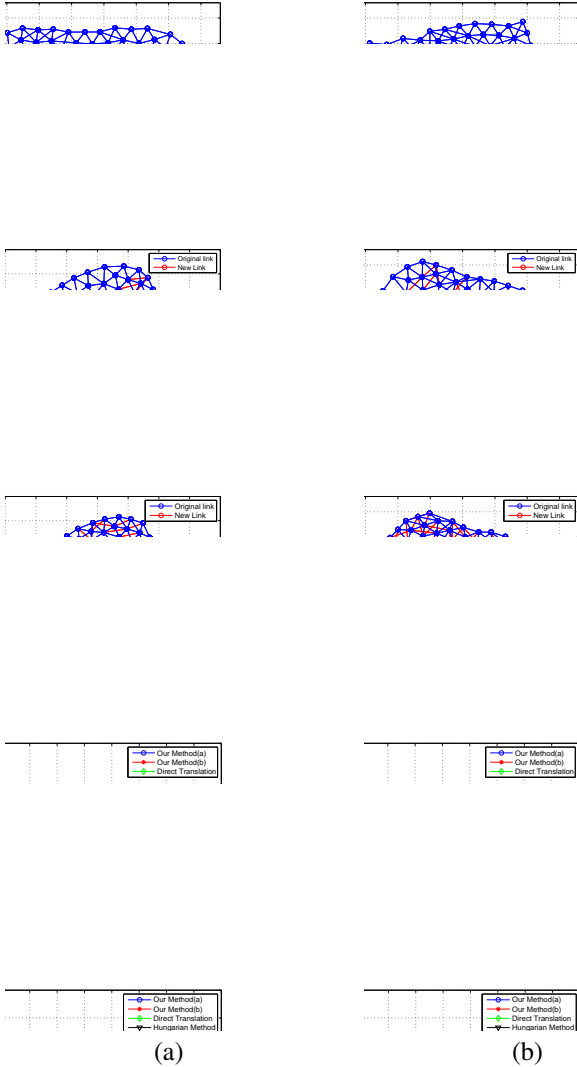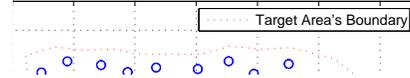
Fig. 6. Mobile robots automatically adjust their deployment density inside a FoI.

FoI. Based on the insights from harmonic map, we propose a modified harmonic map algorithm to find transition path for each mobile robot to target FoI such that both local and global connectivities are maintained. Each mobile robot then follows a specified rule inside the target FoI to do minor adjustment towards its optimal coverage position. Extensive simulations and comparisons with other methods show that the proposed algorithms guarantee global connectivity, and dramatically reduce the broken link ratio at negligible cost of the total moving distance. For the future works, we will consider the optimal marching problem in more complex settings including indoor and 3D surface cases.

REFERENCES

[1] A. Howard, M. Mataric, and G. S. Sukhatme, "Mobile sensor network deployment using potential fields: A distributed, scalable solution to the area coverage problem," in *Proceedings of the 6th International Symposium on Distributed Autonomous Robotics Systems*, 2002.

[2] S. Poduri and G. S. Sukhatme, "Constrained coverage for mobile sensor networks," in *IEEE International Conference on Robotics and Automation*, pp. 165 – 171, 2004.

[3] Y. Zou and K. Chakrabarty, "Sensor deployment and target localization based on virtual forces," in *INFOCOM*, pp. 1293 – 1303, 2003.

[4] E. Martinson and D. Payton, "Lattice Formation in Mobile Autonomous Sensor Arrays," *Lecture Notes in Computer Science*, vol. 3342, pp. 98 – 111, 2005.

[5] G. Wang, G. Cao, and T. F. La Porta, "Movement assisted sensor deployment," *IEEE Transactions on Mobile Computing*, vol. 5, no. 6, pp. 640 – 652, 2006.

[6] M. Ma and Y. Yang, "Adaptive triangular deployment algorithm for unattended mobile sensor networks," *IEEE Transactions on Computers*, vol. 56, pp. 946 – 847, 2007.

[7] T. M. Cheng and A. V. Savkin, "Decentralized control of mobile sensor networks for asymptotically optimal blanket coverage between two boundaries," *IEEE Transactions on Industrial Informatics*, vol. 9, pp. 365 – 376, 2012.

[8] J. Cortes, S. Martinez, T. Karatas, and F. Bullo, "Coverage control for mobile sensing networks," *IEEE Transactions on Robotics and Automation*, vol. 20, no. 2, pp. 243 – 255, 2004.

(a)   (b)

Fig. 5.   The performance of the proposed algorithms on various target FoI models. The first row shows the connectivity graphs of a group of mobile robots deployed in current FoIs. The second row shows the connectivity graphs of the group of mobile robots redeployed in target FoIs following the paths computed by our method (a). Blue color marked edges represent local communication links preserved during the transition to a new FoI. Red color marked edges, on the contrary, are new communication links. The third row shows the connectivity graphs after mobile robots move to optimal coverage positions in target FoIs. The fourth row compares the total moving distance of our methods with others. The fifth row compares the total stable link ratio of our methods with others.

are instructed to redeploy themselves to a new FoI, which may be far from current one. Besides, the new FoI may have complicated and concave boundary shape, with inner obstacles or holes. We show that it is impossible to maintain all local connectivities for general case. We also show that it is a trade-off between preserving connectivities and minimizing the total moving distance to desired optimal positions in the new

[9] M. Schwager, J. Mclurkin, and D. Rus, "Distributed coverage control with sensory feedback for networked robots," in *in Proceedings of Robotics: Science and Systems*, 2006.

[10] F. Li, J. Luo, W. Wang, and Y. He, "Autonomous Deployment for Load Balancing k-Surface Coverage in Sensor Networks," *IEEE Trans. on Wireless Communications*, vol. 14, no. 1, pp. 279 – 293, 2015.

[11] R. Kershner, "The number of circles covering a set," *American Journal of Mathematics*, vol. 61, pp. 665 – 671, 1939.

[12] X. Bai, S. Kumar, D. Xuan, Z. Yun, and T. Lai, "Deploying wireless sensors to achieve both coverage and connectivity," in *Proceedings of the 7th ACM International Symposium on Mobile Ad Hoc Networking and Computing*, pp. 131 – 142, 2006.

[13] X. Bai, Z. Yun, D. Xuan, T. Lai, and W. Jia, "Deploying four-connectivity and full-coverage wireless sensor networks," in *Proc.IEEE INFOCOM*, pp. 906 – 914, 2008.

[14] X. Bai, D. Xuan, Z. Yun, T. Lai, and W. Jia, "Complete optimal deployment patterns for full-coverage and k connectivity ($k \leq 6$) wireless sensor networks," in *Proceedings of the 9th ACM international symposium on Mobile ad hoc networking and computing*, pp. 401 – 410, 2008.

[15] X. Bai, Z. Yun, D. Xuan, W. Jia, and W. Zhao, "Pattern mutation in wireless sensor deployment," in *Proc.IEEE INFOCOM*, pp. 1 – 9, 2010.

[16] H. Kneser, "Losung der aufgabe 41," *Jahresbericht der Deutschen Mathematiker-Vereinigung*, vol. 35, pp. 123 – 124, 1926.

[17] G. Choquet, "Sur un type de transformation analytique generalisant la representation conforme et define au moyen de fonctions harmoniques," *Bulletin des Sciences Mathematiques*, vol. 69, pp. 156 – 165, 1945.

[18] H. Zhou, H. Wu, S. Xia, M. Jin, and N. Ding, "A distributed triangulation algorithm for wireless sensor networks on 2d and 3d surface," in *Proc. of the 30th Annual IEEE Conference on Computer Communications (INFOCOM'11)*, pp. 1053–1061, 2011.

[19] M. Jin, G. Rong, H. Wu, L. Shuai, and X. Guo, "Optimal surface deployment problem in wireless sensor networks," in *Proc. of the 31st Annual IEEE Conference on Computer Communications (INFOCOM'12)*, pp. 2345 – 2353, 2012.

[20] D. Newman, "The hexagon theorem," *IEEE Transactions on Information Theory*, vol. 28, no. 2, pp. 37 – 139, 1982.

[21] S. Lloyd, "Least squares quantization in pcm," *IEEE Trans. Inf. Theor.*, vol. 28, no. 2, pp. 129 – 137, 1982.

[22] Q. Du, M. Emelianenko, and L. Ju, "Convergence of the lloyd algorithm for computing centroidal voronoi tessellations," *SIAM J. Numer. Anal.*, vol. 44, no. 1, pp. 102 – 119, 2006.

[23] H. W. Kuhn, "The hungarian method for the assignment problem," *Naval Research Logistics Quarterly*, vol. 2, pp. 83 – 97, 1955.

[24] H. W. Kuhn, "Variants of the hungarian method for assignment problems," *Naval Research Logistics Quarterly*, vol. 3, pp. 253 – 258, 1956.

[25] J. Edmonds and R. M. Karp, "Theoretical improvements in algorithmic efficiency for network flow problems," *J. ACM*, vol. 19, no. 2, pp. 248 – 264, 1972.

APPENDIX

A. Barycentric coordinates

Barycentric coordinates are triples of numbers (t_1, t_2, t_3) corresponding to masses placed at vertices of v_a, v_b, and v_c of a reference triangle denoted by Δ_{abc}. Barycentric coordinates provide a convenient way to interpolate functions on triangles as long as a function's value is known at vertices.

Let's consider a function f defined on a triangle Δ_{abc} with $f(v_a)$, $f(v_b)$, and $f(v_c)$ known. Denote $Area|\Delta_{abc}|$ the area of triangle Δ_{abc}. The function value of any point p located inside this triangle can be written as a weighted sum of the function value at the three vertices:

$$f(p) = t_1 f(v_a) + t_2 f(v_b) + t_3 f(v_c),$$

where $t_1 = \frac{Area|\Delta_{pbc}|}{Area|\Delta_{abc}|}$, $t_2 = \frac{Area|\Delta_{pca}|}{Area|\Delta_{abc}|}$, and $t_3 = \frac{Area|\Delta_{pab}|}{Area|\Delta_{abc}|}$. It is obvious that t_1, t_2, and t_3 are subject to the constraint:

$$t_1 + t_2 + t_3 = 1.$$

t_1, t_2, and t_3 are called Barycentric Coordinates of Point p on Δ_{ijk}.